III International Conference on Particle-based Methods – Fundamentals and Applications
PARTICLES 2013
M. Bischoff, E. Oñate, D.R.J. Owen, E. Ramm & P. Wriggers (Eds)

MOLECULAR-DYNAMICS SIMULATION OF CONTACT AND FORCE NETWORKS IN FRAGMENTED SEA ICE UNDER SHEAR DEFORMATION

AGNIESZKA HERMAN

University of Gdansk, Institute of Oceanography, Pilsudskiego 46, 81-378 Gdynia, Poland
E-mail: oceagah@ug.edu.pl; http://ocean.ug.edu.pl/∼herman/

Key words: Sea Ice, Granular Model, Force Networks, Shear Deformation, Shear Jamming, Polydispersity

Abstract. Fragmented sea ice can be treated as a strongly polydisperse granular material consisting of approximately disk-shaped grains (ice floes) with power-law size distribution, moving on a two-dimensional sea surface under the influence of external forces (wind, currents, etc.). In this paper, a molecular-dynamics model is used to study the internal stress and the properties of the force networks in sea ice subject to pure shear strain (constant ice concentration). The model exhibits a wide range of behaviors analogous to those observed recently in bidisperse materials, including shear-jammed and fragile states. At certain combinations of ice concentration and strain, the modeled system behaves erratically and undergoes rapid shifts between the jammed and unjammed states, resulting in strong variability in its global characteristics, e.g., the area-average stress and anisotropy of the force networks.

1 INTRODUCTION

Large areas of polar and subpolar oceans are permanently or seasonally covered with ice. Contrary to a multi-year ice pack, seasonal ice cover is usually strongly fragmented and consists of separate floes. However, both ice types are commonly modeled as a continuum, with various versions of the viscous-plastic rheology. Although this approach has been successful in reproducing many large-scale properties of sea ice circulation and dynamics, it has been recognized recently that this 'standard' rheology model is not able to reproduce some of the most crucial aspects of sea ice deformation – its scaling properties and the associated basin-scale propagation of damage due to long-range elastic interactions [1, 2]. Moreover, recent studies suggest the existence of two regimes in the mechanical behavior of sea ice [3, 4, 2], characteristic for the compact central Arctic ice pack (an elastic plate undergoing brittle deformation and damage), and the marginal ice zone (granular material composed of individual ice floes). Whereas the first regime has

been subject of thorough research, very few attempts to directly account for the granular nature of sea ice have been made, most of them aiming at parameterizing its large-scale effects for use in the existing continuous models. For example, a collisional-rheology model was proposed, accounting for the contribution of floe–floe collisions to the internal stress in sea ice [5, 6, 7]. Feltham [8] investigated the role of that rheology model in sea ice dynamics in the marginal ice zone (MIZ). Only recently, discrete-element models have been developed, describing the dynamics of individual ice floes and interactions between them, and providing deeper understanding of granular effects in sea ice and their influence on the emergent properties of the ice cover as a whole [9, 10, 11, 12, 13].

In this work, sea ice is modeled as a two-dimensional (2D) granular material composed of disk-shaped, inelastic grains (ice floes) moving on the sea surface under a prescribed external forcing. The floes have a power-law size distribution, and interact during collisions by means of tangential (friction) and normal (nonlinear Hertzian model, taking into account polydispersity) forces. Numerically, the model is based on the LAMMPS (Large-scale Atomic/Molecular Massively Parallel Simulator) library, and allows for simulating systems of particles within a model domain subjected to various types of deformation (convergence, shear etc.). The model, described in [13], is an extension of earlier, simpler versions based on a hard-disk approximation and an event-driven algorithm [11, 12].

This work investigates the response of sea ice to shear deformation (constant ice concentration A) close to the jamming phase transition, i.e., in conditions relevant, e.g., in MIZ under shoreward winds, or within narrow passages and straits. The analysis concentrates on the statistical properties of the contact and force networks and on the resulting internal stress. Although the model has been designed to represent sea ice, the results presented here are relevant from two different perspectives. Firstly, they provide insight into little understood granular effects on the dynamics of shear-strained sea ice. Secondly, recent experimental studies suggest very rich phenomenology of sheared granular materials close to the jamming phase transition [14, 15]. The number of analogous numerical studies reproducing that behavior has been very limited. Except for the very strong polydispersity, the model used here corresponds in its most important features to the experimental setup of the above-mentioned studies: it describes disk-shaped grains (ice floes) moving in 2D on a frictional substrate (sea surface), with frictional forces typically much smaller than the grain–grain interaction forces. Thus, the results presented here provide additional insight into the behavior of sheared, polydisperse granular materials in general.

2 MODEL DESCRIPTION

2.1 Model assumptions and equations

The model used for the simulations in this paper has been described in detail in [13]; therefore, here only a brief summary of the underlying assumptions and the governing equations is given.

The modeled system consists of $i = 1, \ldots, N$ disk-shaped floes with radii r_i, thickness

h_i and a constant density ρ. The general form of the equations for the linear and angular momentum of the ith floe is:

$$m_i \frac{d\mathbf{u}_i}{dt} = -m_i f \mathbf{k} \times \mathbf{u}_i + \int_{S_i} \check{\mathbf{f}}_{s,i} \mathrm{d}s + \int_{V_i} \check{\mathbf{f}}_{b,i} \mathrm{d}v + \sum_{j \in \mathcal{C}_i(t)} \hat{\mathbf{F}}_{ij,n} \tag{1}$$

and:

$$m_i \frac{r_i^2}{2} \frac{d\omega_i}{dt} = \mathbf{k} \cdot \left[\int_{S_i} \mathbf{r} \times \check{\mathbf{f}}_{s,i} \mathrm{d}s + \int_{V_i} \mathbf{r} \times \check{\mathbf{f}}_{b,i} \mathrm{d}v + \sum_{j \in \mathcal{C}_i(t)} \mathbf{r}_{ij} \times \hat{\mathbf{F}}_{ij,t} \right], \tag{2}$$

where $m_i = \pi \rho h_i r_i^2$ is the mass of the floe, $\mathbf{u}_i$ – velocity of its mass center, ω_i – its angular velocity, t denotes time, f – the Coriolis parameter, $\mathbf{k}$ – a unit vector pointing vertically upward, S_i and V_i – the upper/lower surface area and volume of the floe, $\mathbf{r}$ – the distance from the floe's center, and $\mathbf{r}_{ij}$ – a vector pointing from the center of floe i to the contact point with floe j. Finally, $\mathcal{C}_i(t)$ denotes the set of floes that are in contact with floe i at a given time instance. For $j \in \mathcal{C}_i$, $\hat{\mathbf{F}}_{ij,n}$ and $\hat{\mathbf{F}}_{ij,t}$ are the normal and tangential components, respectively, of the floe–floe interaction force, calculated based on the Hertzian contact model (see, e.g., [16, 17]). The external (ocean/atmosphere) forcing acting on the floes is expressed in terms of the density of the surface and body forces, denoted with $\check{\mathbf{f}}_{s,i}$ and $\check{\mathbf{f}}_{b,i}$, respectively.

The previous works [11, 12, 13] stressed the importance of the size-dependent response of individual ice floes to the forcing acting on them, relevant at low and medium ice concentrations. However, the focus of this paper is on a compact, slowly moving ice cover at or close to the jammed state. Therefore, the simulations described further were performed with a simplified set of equations, without the form-drag terms responsible for the size-dependent response (see [13] for comparison). Furthermore, it is assumed that both the wind speed and the current speed are zero, and that the Coriolis term can be omitted within confined regions considered here. The ocean is at rest and linearized formulae are used for the ice–ocean friction term. Thus, equations (1), (2) simplify to:

$$m_i \frac{d\mathbf{u}_i}{dt} = -\pi r_i^2 \rho_w C_{hw} \mathbf{u}_i + \sum_{j \in \mathcal{C}_i(t)} \hat{\mathbf{F}}_{ij,n} \tag{3}$$

and

$$m_i \frac{r_i^2}{2} \frac{d\omega_i}{dt} = -\pi \frac{r_i^4}{2} \rho_w C_{hw} \omega_i + \mathbf{k} \cdot \sum_{j \in \mathcal{C}_i(t)} \mathbf{r}_{ij} \times \hat{\mathbf{F}}_{ij,t}, \tag{4}$$

where ρ_w denotes the water density and C_{hw} – the water–ice drag coefficient.

As described in [13], the model is based on the LAMMPS (Large-scale Atomic/Molecular Massively Parallel Simulator) library [18] (see also `http://lammps.sandia.gov/`), designed for simulating large systems of interacting objects (particles, molecules, etc.). For

Table 1: Physical and numerical model parameters used in the simulations

Parameter	Symbol	Value	Units
Ice density	ρ	910	kg/m^3
Water density	ρ_w	1025	kg/m^3
Water–ice skin-drag coef.	C_{hw}	$1.0 \cdot 10^{-3}$	m/s
Ice thickness	h	1.5	m
FSD slope	α	1.8	—
Mean floe radius	$\bar{r}$	4.0	m
Elastic modulus of sea ice	E	$9.0{\cdot}10^9$	Pa
Poisson's ratio	ν	0.33	—
Static yield criterion	μ	0.7	—
No. of floes	N	20000	—
Time step	Δt	0.002	s

the purpose of sea ice modeling, LAMMPS has been extended to disk-shaped particles moving within two-dimensional domains. For all N floes, the Newton equations of motion (1),(2) – or, in this particular case, (3),(4) – are solved by means of the velocity-Verlet integrator.

2.2 Model configuration for shear-deformation simulations

The calculations described in this paper were performed in pure shear conditions, with the ice concentration A kept constant during any given simulation. The model domain was rectangular, with length L_x, width $L_y = L_x/2$, and surface area $S = L_x L_y = \pi \sum_{i=1}^{N} r_i^2 / A$. Periodic boundary conditions were used along the x-axis. The floes along the lower model boundary were defined as 'frozen', i.e., their velocity was set to zero. The floes along the upper model boundary had a prescribed velocity $\mathbf{u}_i = [u_b, 0]$. Thus, the strain rate of the modeled system was $\epsilon = u_i / L_y$. The simulations were performed for a range of values of ice concentration $A \in [0.890, 0.908]$ and strain rate $\epsilon \in [1.5 \cdot 10^{-4}, 7.5 \cdot 10^{-4}]$ s^{-1} (corresponding to $u_b \in [0.2, 1.0]$ m/s), for a sample of $N = 20000$ floes with radii r_i drawn from a power-law distribution with an exponent $\alpha = 1.8$ and mean $\bar{r} = 4$ m (values corresponding to those observed in sea ice in the Weddell Sea [19]). A complete list of the model parameters can be found in Table 1.

3 MODELING RESULTS

As can be expected, the area-averaged internal stress in the modeled system of ice floes increases with ice concentration. In analogous simulations under pure convergence, the system undergoes a jamming phase transition when the ice concentration A approaches a limiting value A_J from below. For the system analyzed here, $A_J \sim 0.918$ (wide, power-law type particle-size distributions allow denser packing fractions, and hence this value

is higher than, e.g., 0.83 reported for bidisperse systems [14]). The jamming transition manifests itself with a rapid increase of pressure, fraction of non-rattler floes (i.e., floes with at least two contacts) and the mean contact number [13]. As will be illustrated below, under the shear deformation considered here, the model behavior close to A_J is more complex, with large-scale system characteristics undergoing erratic, often very rapid changes, even under constant domain-scale strain rate ϵ.

Figure 1 shows the patterns of floe–floe contact forces in situations corresponding to three different states of the system. At high ice concentration and/or strong shear strain, the system develops a dense force network spanning the whole model domain and remains in a jammed state during the whole simulation time (Fig. 1a). At lower A and/or ϵ, jamming does not occur and, although local regions of higher pressure and the associated forces may develop (Fig. 1c), the domain-wide internal stress remains at low levels, typically a few orders of magnitude lower than in the jammed state (Fig. 2c,d). Both in the jammed and unjammed states, the large-scale system characteristics – including the mean contact number η_c and the anisotropy of the force network η_a, the pressure p and shear stress τ, and the principal angle θ_p (Fig. 2) – remain relatively stable in time, and the system recovers fast from short 'rearrangement' events that sporadically take place.

From the point of view of the dynamics of the system, perhaps the most interesting behavior is observed in between the two extremes described above. The system undergoes rapid changes and shifts from unjammed to jammed state and *vice versa*. Between those two extremes, the force networks often have a fragile, 'openwork' structure, with relatively large unjammed areas where the stress remains very low, and with forces transmitted *via* long 'strands' of approximately linearly aligned floes. As in the case of fragile states observed recently [14], those force networks may span the whole model domain in only one (compressive) direction, giving the material anisotropic strength in response to deformation. The present results suggest that, even in constant-strain conditions, the fragile states are short-lived, at least in the range of A and ϵ combinations analyzed here. Interestingly, force networks obtained in simulations with wind and floe-size-related effects [13] have many properties analogous to those observed here.

The rapid, erratic changes of the system state are closely related to the very strong polydispersity of the particles (floes) building that system. With the power-law size distribution, the largest floes occupy a substantial part of the available surface area (even with increasing system size N) and it is their locations and relative movement that has a deciding influence on the system as a whole. Sub-regions of the model domain that at a given time instance are filled with small floes can change their shape – and thus react to deformation – more easily than assemblies of large floes. In many respects, assemblies of very small floes act as a plastic, easily deformable 'filler' occupying empty spaces between very large floes. An analysis of animations illustrating the time evolution of the modeled system reveal that the rapid jamming and un-jamming events tend to be associated with reorganization of the positions of the largest floes.

4 DISCUSSION AND CONCLUSIONS

Shear strain is the dominant mode of deformation of sea ice in large parts of the Arctic (e.g., [2]). Even though the simulations described in this paper are highly idealized, they illustrate some very important features, inherent in strained polydisperse granular systems and crucial for our understanding of the behavior of a compact, fragmented ice cover in general and its response to shear deformation in particular. The results are relevant for fragmented sea ice within confined basins where, due to limited divergence, the ice concentration remains relatively constant, and – obviously – for situations when the internal stress in the ice does not exceed the ice strength, as the present 2D model does not include ridging or breaking of the ice floes. One of the important, practically relevant directions of research on sea ice has been on its rheology. Models relating the internal stress σ in the ice in response to strain, $\sigma(\epsilon)$, are a fundamental part of all large-scale numerical models of sea ice formulated within the continuum framework. The results of discrete-element models, as those presented here, help to reveal the complex nature of that relationship, especially in situations when the granular effects become important. As shown in Figs. 3 and 4, even in idealized simulations with constant A and ϵ, the area-average internal pressure varies substantially, in some cases by a few orders of magnitude. At high A, when the system remains jammed or close to jamming, the probability density functions (pdfs) of p have a clear peak, but are strongly skewed, with long tails towards lower values of pressure. The asymmetry of the pdfs decreases with decreasing A. An important conclusion is that, even in 'stationary' conditions considered here, the instantaneous pressure or shear stress cannot be expressed as a function of A and ϵ. This is especially true in unjammed states, characterized by $\eta_c < 3$ (Fig. 4). These results are in agreement with field observations that reveal intermittent character of the internal stress in sea ice (both in terms of its amplitude and direction), unrelated to the variability of the external forcing [20, 21].

REFERENCES

[1] L. Girard, J. Weiss, J.M. Molines, B. Barnier, and S. Bouillon. Evaluation of high-resolution sea ice models on the basis of statistical and scaling properties of Arctic sea ice drift and deformation. *J. Geophys. Res.*, 114:C08015, 2009.

[2] J. Weiss. *Drift, Deformation, and Fracture of Sea Ice: A Perspective Across Scales.* Springer Briefs in Earth Sciences. Springer, 2013. 83 pp.

[3] J. Weiss and E.M. Schulson. Coulombic faulting from the grain scale to the geophysical scale: lessons from ice. *J. Physics D*, 42:214017, 2009.

[4] J. Weiss, E.M. Schulson, and H.L. Stern. Sea ice rheology from in-situ, satellite and laboratory observations: Fracture and friction. *Earth Planetary Sci Lett.*, 255:1–8, 2007.

[5] H.H. Shen, W.D. Hibler III, and M. Leppäranta. On the rheology of a broken ice field due to floe collision. *MIZEX Bulletin III, USACREL Special Report 84-28*, pages 29–34, 1984.

[6] H.H. Shen, W.D. Hibler III, and M. Leppäranta. On applying granular flow theory to a deforming broken ice field. *Acta Mechanica*, 63:143–160, 1986.

[7] Q. Lu, J. Larsen, and P. Tryde. On the role of ice interaction due to floe collisions in marginal ice zone dynamics. *J. Geophys. Res.*, 94(C10):14525–14537, 1989.

[8] D.L. Feltham. Granular flow in the marginal ice zone. *Phyl. Trans. Royal Soc. A*, 363:1677–1700, 2005.

[9] R. Gutfraind and S.B. Savage. Marginal ice zone rheology: Comparison of results from continnum-plastic models and discrete-particle simulation. *J. Geophys. Res.*, 120:12647–12661, 1997.

[10] M.A. Hopkins and A.S. Thorndike. Floe formation in Arctic sea ice. *J. Geophys. Res.*, 111:C11S23, 2006.

[11] A. Herman. Molecular-dynamics simulation of clustering processes in sea-ice floes. *Phys. Rev. E*, 84:056104, 2011.

[12] A. Herman. Influence of ice concentration and floe-size distribution on cluster formation in sea ice floes. *Cent. Europ. J. Phys.*, 10:715–722, 2012.

[13] A. Herman. Numerical modeling of force and contact networks in fragmented sea ice. *Annals Glaciology*, 54:114–120, 2013.

[14] D. Bi, J. Zhang, B. Chakraborty, and R.P. Behringer. Jamming by shear. *Nature*, 480:355–358, 2011.

[15] J. Zhang, T.S. Majmudar, A. Tordesillas, and R.P. Behringer. Statistical properties of a 2d granular material subjected to cyclic shear. *Granular Matter*, 12:159–172, 2010.

[16] N.V. Brilliantov, F. Spahn, J.-M. Hertzsch, and T. Pöschel. Model for collisions in granular gases. *Phys. Rev. E*, 53:5382–5392, 1996.

[17] T. Schwager. Coefficient of restitution for viscoelastic disks. *Phys. Rev. E*, 75:051305, 2007.

[18] S. Plimpton. Fast parallel algorithms for short-range molecular dynamics. *J. Comp. Phys.*, 117:1–19, 1995.

[19] A. Steer, A. Worby, and P. Heil. Observed changes in sea-ice floe size distribution during early summer in the western Weddell Sea. *Deep-Sea Res. II*, 55:933–942, 2008.

[20] J. Weiss and D. Marsan. Scale properties of sea ice deformation and fracturing. *C. R. Physique*, 5:735–751, 2004.

[21] J. Weiss. Intermittency of principal stress directions within Arctic sea ice. *Phys. Rev. E*, 77:056106, 2008.

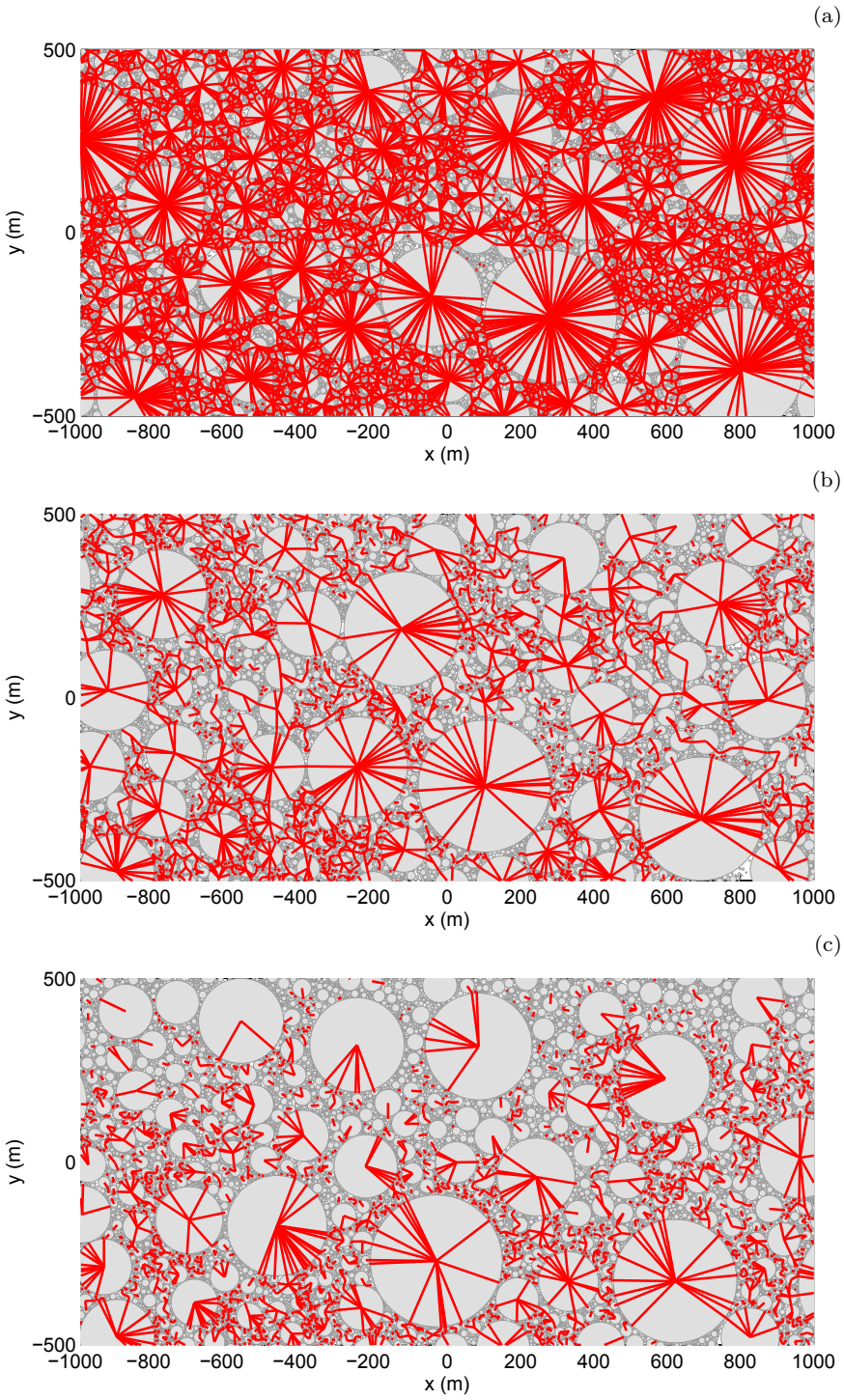

Figure 1: Snapshots of fragments of the model domain, showing the pattern of instantaneous forces between ice floes during simulations with: $A = 0.908$ and $u_b = 1.0$ m/s (a); $A = 0.905$ and $u_b = 0.5$ m/s (b); $A = 0.905$ and $u_b = 0.2$ m/s (c). For each floe i, a line is drawn from its center to the center of floe j if $j \in C_i(t)$.

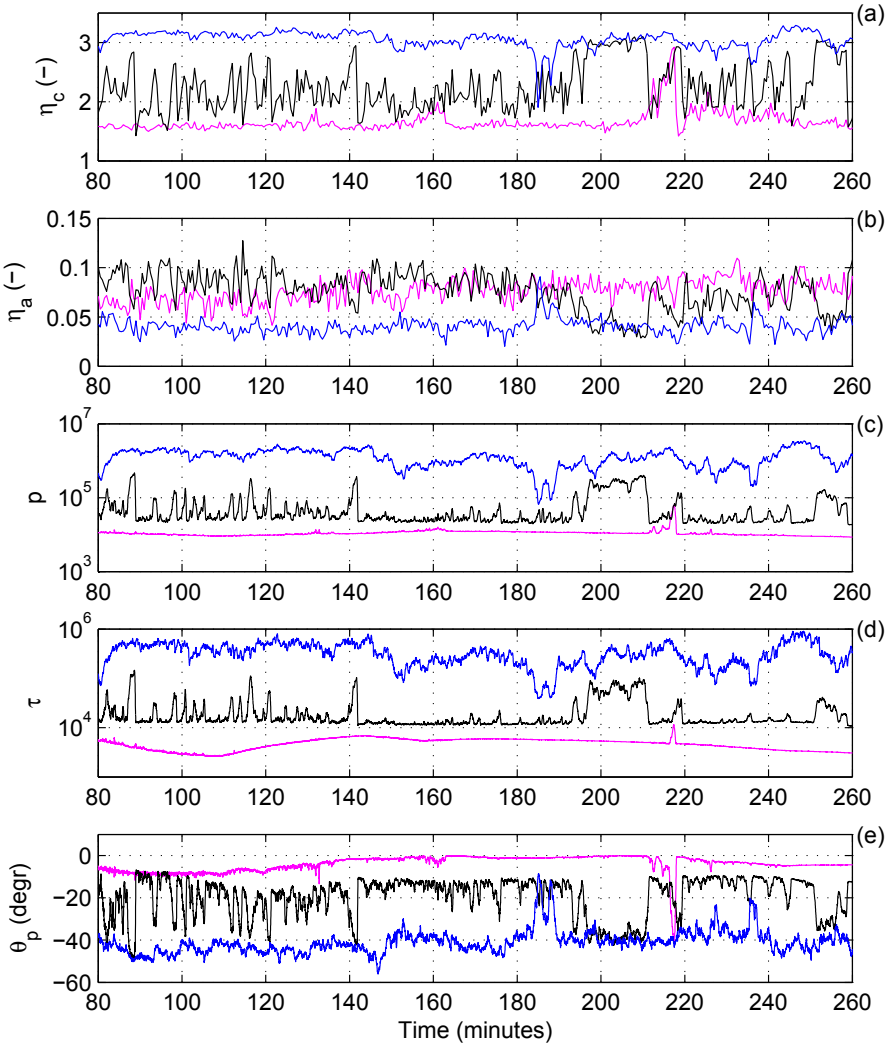

Figure 2: Time series of the average contact number η_c (a), force-network anisotropy η_a (b), pressure p (c), shear stress τ (d), and the principal angle θ_p (e) during simulations with: $A = 0.908$ and $u_b = 1.0$ m/s (blue); $A = 0.905$ and $u_b = 0.5$ m/s (black); $A = 0.905$ and $u_b = 0.2$ m/s (magenta).

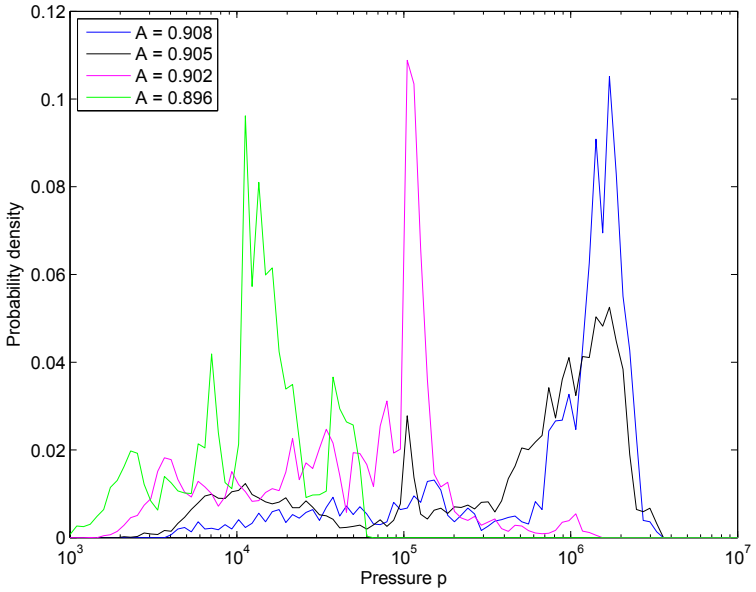

Figure 3: Probability distribution functions of the internal pressure p in sea ice subject to a constant strain rate ϵ (determined by $u_b = 1.0$ m/s). Results of four simulations with different ice concentration A. Note that the x-axis is logarithmic.

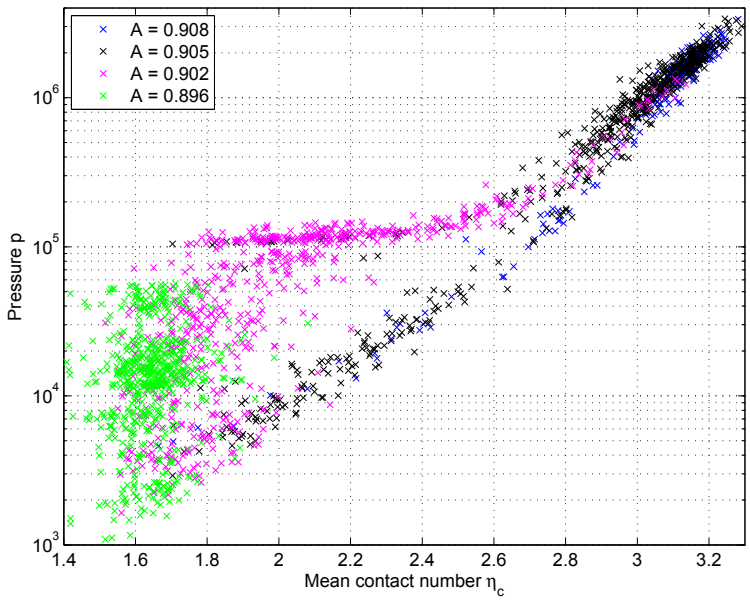

Figure 4: Relationship between η_c and p for four model runs with $u_b = 1.0$ m/s and different ice concentration A.